Springer

Journal of
Mechanical
Science and
Technology

Journal of Mechanical Science and Technology 22 (2008) 946~956

www.springerlink.com/content/1738-494x

Transient elastohydrodynamic lubrication film thickness in sliding and rolling line contacts

Siyoul Jang*

School of Mechanical and Automotive Engineering, Kookmin University
861-1, Chungnung-dong, Sungbuk-gu, Seoul, 136-702, Korea

(Manuscript Received September 10, 2007; Revised January 24, 2008; Accepted January 31, 2008)

Abstract

The contact behavior between cam and follower is greatly influenced by the kinematics and dynamics of the whole valve train system. This is the reason that both shape and thickness of the fluid film in the contact gap are mainly determined by applied loads and relative contact speeds as well as the curvatures of contacting elements. Most of the studies about lubricant film behavior between cam and follower have been performed without a consideration of transient effects in the contact gap. For the computational difficulties of transient effects, most contact conditions such as relative contacting speeds have been regarded as quasi-steady state during the whole operating cycle.

In this work, in order to obtain stable convergence, a multigrid multi-level method is used for the computation of load capacity in the lubricant film. Nonlinear valve spring dynamics are also considered in the same way as Hanachi's. From the computational results, transient EHL film thicknesses under the conditions of different contact geometries are computed for a pushrod type valve train system during an engine cycle. Several results show the squeeze film effect, which is generally not found with conventional EHL computations of the cam and follower contact. The results are also compared with those by the Dowson-Hamrock (D-H) formula, which does not consider the dynamic film effect. Without the dynamic film effect as in D-H's formula, the minimum film thickness is highly dependent on the entraining lubricant velocity, whereas the minimum film thickness including the squeeze film effect is dependent on the applied load.

Keywords: Elastohydrodynamic lubrication (EHL); Multigrid multi-level method; Squeeze film effect; Valve train system; Fluid film thickness

1. Introduction

The lifts of intake and exhaust valves are strongly influenced by the stiffness and damping of valve springs and valve seats, masses and geometries of components, and frictional behavior of contacting components. In general, a valve lift has a similar shape to the cam displacement at low engine speed, but at high speed (over 3000rpm) it does not depend only on the shape of the cam profile. Among the components in a valve train system, the valve spring has the most influential effect on the pattern of the valve lift. Particularly, a higher camshaft rotational speed generates unexpected valve motion which is caused by viscous or coulomb-damping effects in the valve spring, and subsequently it makes the spring stiffness highly nonlinear. On the other hand, a lower camshaft speed gives a very similar shape of valve lift to cam displacement [1]. These effects mainly result in nonlinear kinematics and dynamics of a valve train system as well as provide unrelated prediction to experimental data, regardless of the types of valve train systems such as pushrod, center pivot finger, cam-in-head, end pivot finger, and direct acting types [2-4].

Both pattern and thickness of the fluid film between cam and follower are mainly determined by applied loads and relative contacting speeds. The cam

*Corresponding author. Tel.: +82 2 910 4831, Fax.: +82 2 910 4839
E-mail address: jangs@kookmin.ac.kr
DOI 10.1007/s12206-008-0124-3

contact behavior with a follower is greatly influenced by the kinematics and dynamics of the whole valve train system. Most of the studies about the lubricant behavior between cam and follower have been performed without a consideration of nonlinear dynamics [5] among the components of the valve train system. Without these non-linear characteristics, the computational results give simple kinematic similarities. That is, the contact force between cam and follower is computed only with the geometrical variation. With the effects of nonlinear loading condition in the valve train system, especially from the valve spring characteristics, the elastic deformation over the contact region becomes another influential factor regarding the prediction of load capacity in lubricant film. Due to the computational difficulty, many numerical predictions of lubricant behavior between the cam and follower do not fully consider the effects of nonlinear valve spring dynamics and the elastic deformation [6] on the surface over cam and follower caused by the concentrated pressure under the nonconformal contacting geometry.

Among the computational researches about EHL study, the contact conditions such as relative contacting speeds are regarded as quasi-steady state during the whole engine cycle for simple computation. [7-9] Therefore, in most such computational researches about valve train contacts the film thickness has been evaluated merely with the curve fitting formula by Hamrock and Dowson's [6], which comes from the computational results of steady state condition.

In this work, in order to obtain convergence and stability, a multigrid multi-level method is used for the computation of load capacity in the lubricant film. [10] This method is recently in wide use for solving the nonlinear partial differential equations for its characteristics of convergence stability. Nonlinear valve spring dynamics are considered in the same way as Hanachi's [11], and transient EHL film thicknesses for the cases of flat and rolling followers are computed in the pushrod type valve train system [12, 13].

2. Analysis of contact geometries for flat and rolling followers

The magnitude of the valve lift can be generated by a four-power polynomial, which is described below Eq. (1) in order to get the desired functional requirement of flow rates into the combustion cylinder. For the given valve lift, l_{cam} [8] whether it is for flat or rolling follower, the cam profiles are generated by the kinematic investigation of the pushrod type valve train system.

$$l_{cam} = 9.48\left(1 - 1.242\left(\frac{\theta}{60}\right)^2 + 0.255\left(\frac{\theta}{60}\right)^{12} - 0.115\left(\frac{\theta}{60}\right)^{68} + 0.102\left(\frac{\theta}{60}\right)^{70}\right) \quad (1)$$

In general, the frictional behavior in the valve train system is known to be diminished by adopting a rolling follower instead of a flat one. Therefore, the load capacities of lubricant films between cam and flat/roller followers are computed for the pushrod type valve train system in this work. Each basic geometrical dimension of the valve train system using flat and rolling follower is all the same for the fixed amount of valve lift (Fig. 1). However, due to the contact geometries between cam and follower around the contact spot that are totally different from each

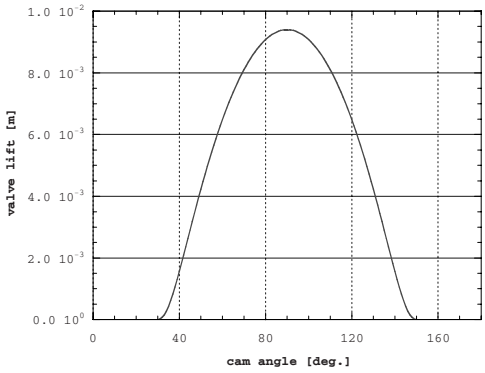

Fig. 1. Valve lifts for flat and rolling followers.

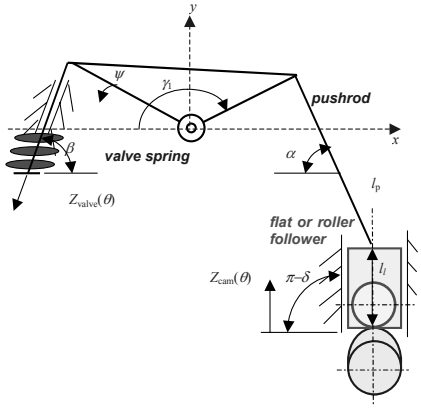

Fig. 2. Schematic diagram of pushrod type valve train system.

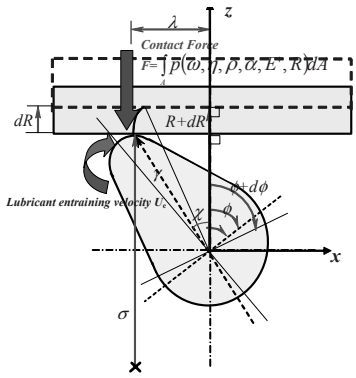

Fig. 3. Contact geometry between cam and flat follower.

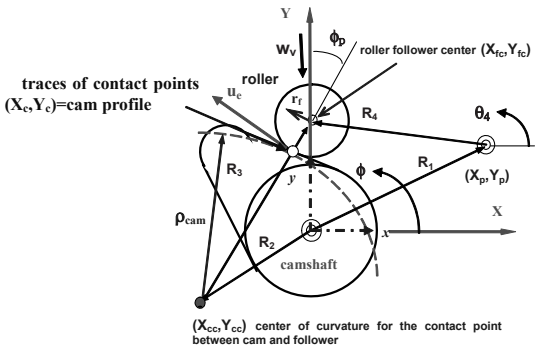

Fig. 4. Contact geometry between cam and rolling follower.

other, the cam profile shape to the flat follower is not generated in the same way as that to the rolling one.

The relative contact velocity between cam and follower is another important parameter for the computation of lubricant load capacity, because it determines the entraining velocities of the lubricant into the gap. In this study, a perfectly flat follower type, Stone [13] (Fig. 2) is selected for simplicity of computation. The contact geometry with the curvature-faced follower which is rather complex will be easily investigated with the results of our work. The instantaneous radius of curvature for the contact between cam and flat follower in Fig. 3, is described as below: [13]

$$\sigma = \frac{\left\{\gamma^2 + \left(\frac{d\phi}{d\chi}\right)^2 \left(\frac{d\rho}{d\phi}\right)^2\right\}^{\frac{3}{2}}}{\gamma^2 - \gamma\frac{d\gamma}{d\phi}\frac{d^2\phi}{d\chi^2} - \gamma\frac{d^2\gamma}{d\phi^2}\left(\frac{d\phi}{d\chi}\right)^2 + 2\left(\frac{d\gamma}{d\phi}\right)^2\left(\frac{d\phi}{d\chi}\right)^2} \quad (2)$$

where,

$$\gamma = \sqrt{\left\{R^2 + \left(\frac{dR}{d\phi}\right)\right\}} \quad (3)$$

and

$$\chi = \phi + \tan^{-1}\left(\frac{1}{R}\frac{dR}{d\phi}\right). \quad (4)$$

Using the values of γ and χ, the distance and angle from the center of cam to the contact point, respectively, the velocity components at the contacting point between cam and flat follower are given by the following:

$$u_c = \gamma\omega\cos(\chi - \phi), \quad (5)$$

$$u_t = \frac{d\lambda}{dt} = \left(\frac{d^2R}{d\phi^2}\right)\omega. \quad (6)$$

These are the velocity components parallel and axial to tappet surface, respectively. The sliding velocity, u_s , and the entraining velocity of lubricant, u_e , are expressed as below:

$$u_s = u_c - u_t, \quad (7)$$

$$u_e = \frac{u_c + u_t}{2}. \quad (8)$$

The entraining velocity of the lubricant varies depending on the curvature of the follower at the contacting point, which, for simplicity, is considered a straight line in this study. For the flat follower, a kinematic study of the valve train system is similarly performed according to the methods (Paranjpe [4]).

However, this investigation cannot be the same as the kinematic investigation of a rolling follower, because the contact mechanism of the rolling follower has a different contact geometry from that of a flat follower around the contact spots. The contact locus (X_c, Y_c) between cam and rolling follower is computed by the four-linkage system (Fig. 4) by the following vector summation, Eq. (9) [15].

$$\vec{R}_2 + \vec{R}_3 - \vec{R}_4 - \vec{R}_1 = 0 \quad (9)$$

Differentiating Eq. (9) with respect to the angle of camshaft rotation ϕ gives Eqs. (10) and (11) in x and y components.

$$-R_2\sin\theta_2 - \frac{\partial\theta_3}{\partial\phi}R_3\sin\theta_3 + \frac{\partial\theta_4}{\partial\phi}R_4\sin\theta_4 = 0 \quad (10)$$

$$R_2\cos\theta_2 + \frac{\partial\theta_3}{\partial\phi}R_3\cos\theta_3 - \frac{\partial\theta_4}{\partial\phi}R_4\cos\theta_4 = 0 \quad (11)$$

The center (X_{CC}, Y_{CC}) of curvature of the camshaft at the point of contact is obtained as follows: if there is no offset for the roller center from the line to the

center of base circle of cam profile, then

$$X_{CC} = X_{fc} - R_3 \cos\theta_3 \tag{12}$$

$$Y_{CC} = Y_{fc} - R_3 \sin\theta_3 \tag{13}$$

Assuming that there is no slipping between cam and follower, the relative motion of these two components of contact velocities is described as below.

$$\rho_{cam}\left(\frac{\partial\phi}{\partial t} - \frac{\partial\theta_3}{\partial t}\right) = -r_f\left(\frac{\partial\theta_f}{\partial t} - \frac{\partial\theta_3}{\partial t}\right) \tag{14}$$

Therefore, the entraining velocity of the lubricant is obtained from the following Eq. (15).

$$u_e = \rho_{cam}\left(\frac{\partial\phi}{\partial t} - \frac{\partial\theta_3}{\partial t}\right) = -r_f\left(\frac{\partial\theta_f}{\partial t} - \frac{\partial\theta_3}{\partial t}\right) \tag{15}$$

The cam profile for the rolling follower with the assumption that there is no slipping between cam and rolling follower can be obtained from kinematic simulation after computing the contact point locus (X_c, Y_c) as below with zero offset along the camshaft-roller line.

The traces of the roller center (X_{fc}, Y_{fc}) as the valve lifts are in the line of the y-axis as shown in Fig. 4 and express the sum of cam radius R_c, valve lift l_{cam} and roller radius R_r.

$$X_{fc} = 0 \tag{16}$$

$$Y_{fc} = R_c + R_r + l_{cam} \tag{17}$$

Therefore, the cam profile is the transformed trace of the (X_{fc}, Y_{fc}) as the function of the cam shaft rotation.

$$\begin{bmatrix} X_c \\ Y_c \end{bmatrix} = \begin{bmatrix} \cos\theta & \sin\theta \\ -\sin\theta & \cos\theta \end{bmatrix} \begin{bmatrix} X_{fc} \\ Y_{fc} \end{bmatrix} \tag{18}$$

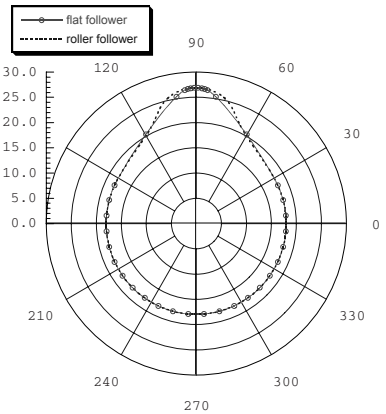

Fig. 5. Generated cam profiles by flat and rolling followers.

The generated cam profiles by tracing the contact points from the kinematic investigation of the valve train linkage system for flat and rolling followers are shown in Fig. 5, where the cam for the rolling follower has a unique concaved shape around 70° and 90° of the camshaft angles.

The effect of viscous damping on the valve spring causes the nonlinear characteristics of valve lift motions, which in turn makes the contact force between cam and follower very unpredictable. The other damping effects from other components by contacting are not considered in this computation, because experimental data by previous researches [1-3, 5] do not show good coincidence with simulation works. However, the distributed viscous damping and nonlinear stiffness of the valve spring are too large to be ignored. These are regarded as major factors for contacting forces between cam and follower in this computation. The distributed damping and stiffness are numerically computed by the Hanachi method [11].

The elastic force at the end of valve spring that has total length, L is given by:

$$F_s = F_e(\xi)\big|_{\xi=L} = -KL\frac{\partial y}{\partial \xi}\bigg|_{\xi=L} \tag{19}$$

where

$$K = \frac{G'd^4}{64r^3N_c}. \tag{20}$$

The analytical expression for the motion of viscous damped spring in Fig. 3 is given by the following equation:

$$\alpha'^2\frac{\partial^2 y}{\partial \xi^2} = \frac{\partial^2 y}{\partial t^2} + \beta\frac{\partial y}{\partial t} \tag{21}$$

where

$$\alpha' = d\sqrt{\frac{G'}{\rho'\left(8r^2 + d^2\right)}}, \tag{22}$$

$$\beta = \frac{32r^2\varepsilon}{\pi d^2\rho'\left(8r^2 + d^2\right)}, \tag{23}$$

and $$\varepsilon = \frac{4\mu F(\xi)}{\pi\omega Y_0}. \tag{24}$$

As it is shown in Eq. (19), the elastic spring force is strongly dependent on the term $\partial y/\partial\xi$, which could be obtained by solving the wave Eq. (21). The elastic deformation y is not only a function of curvilinear length, ξ, but that of loading frequency, t. Therefore, the spring force shows considerable nonlinear behavior at high speeds of loading which come from high

Table 1. Dimensions of valve train components.

Cam base circle	18mm	Lubricant G	5300.9
l_1	27.39mm	Spring G'	8.3×10^{10} N/m^2
l_p	120.0mm	γ_1	145°
R_1	45mm	Valve lift	8.47mm
η_0 (lubricant vis.)	0.0411Pas	Press-visco coeff. α	2.42×10^{-8}m^2/N
Rolling follower radius	10mm	Young's modulus	200×10^9N/m^2
Spring diameter	5.166mm	Spring roll R	15.56mm

rotational speed of camshaft. This cannot be verified with the conventional static coil spring model and it causes a serious error in the estimation of valve displacement [11]. Although the spring force is very nonlinear due to the imposing speed of the loads, the spring displacement itself is fixed by the kinematic relationship due to the valve lift. However, the coil spring forces are varied with the internal vibration mode according to the loading frequency even if there are no imposing displacements. Therefore, all other kinematic relationships among the valve train components are fixed and the entraining velocity of the lubricant is dependent only on the geometrical relationship of the valve train system.

With the consideration of distributed damping and stiffness in the valve spring, the spring force is computed as a function of valve lift, y. The valve lift is computed by investigating the interactions among the components in the valve train linkage system such as valve guide, rocker arm, pushrod, follower and cam. The kinematic investigation of these components is performed as the way of Goenka [1] for the valve train system of pushrod type. The detail dimensions of the components in this work are listed in Table 1. With the computation of valve lift y, the contacting force between cam and follower could be obtained. In this computation the damping effects among the contacting components except in valve spring are ignored. This is the reason that they are small enough to be suppressed by the damping of valve spring and hard to be characterized in magnitude. What is more, simulation and experimental works show that there are rare coincidences in the damping characteristics.

3. Analysis of the dynamic behavior of lubricant between cam and follower

Most of the studies for the computation of EHL film thickness have been performed with the viewpoint of steady loading conditions because of computational simplicity. At each contact point between cam and follower, the loading condition changes according to the rotational speed of a camshaft during a cycle and, therefore, the dynamic loading effects should not be ignored. The mathematical formulation of EHL film thickness between cam and follower under dynamic loading condition is described by the following Reynolds equation:

$$\frac{\partial}{\partial x}\left(\frac{\rho h^3}{12\eta}\frac{\partial p}{\partial x}\right)+\frac{\partial}{\partial y}\left(\frac{\rho h^3}{12\eta}\frac{\partial p}{\partial y}\right)=u_e\frac{\partial(\rho h)}{\partial x}+\frac{\partial(\rho h)}{\partial t} \quad (25)$$

The second term of the right hand side in Eq. (25) reflects the dynamic loading condition that is usually ignored in the conventional analysis of EHL film thickness. However, the contact geometry, entraining velocity of lubricant and applied load vary as the rotation of camshaft speed, which means that the film thickness is also a function of loading frequency. Most of the conventional EHL studies have ignored this effect, and therefore the minimum film thickness for EHL contacts is computed simply by using Dowson-Hamrock's [8] curve fitting formula, Eq. (26) for its ease of computation. However, the formula is based on the condition of steady loading state and never includes the squeeze film effect that very frequently occurs in real engineering contacts. Ignoring the dynamic effect in the computation of EHL film shape shows a large difference from other experimental investigations, so that the estimation with only steady loading condition leads to a misinterpretation of lubrication behavior between cam and follower.

$$h^*=\frac{h_{\min}}{R}=1.714W^{*-0.128}U^{*0.694}G^{0.568} \quad (26)$$

The contact regions between cam and follower have elliptical features because both cam and follower have small curvatures ($1/\rho<<0$) along the camshaft axis whether it is flat or rolling type. However, the contact shape between cam and follower is generally considered as line contact in most computational EHL analyses, because the ratio of major and minor axes of contact area is relatively large. For this reason, the second term of the left hand side of Eq. (25) is ignored in this work and the elliptical contact is regarded as line contact, which saves much computing time in both calculations of elastic deformations and EHL film pressures. The elastic deformation for the line contact is described by the following form: [6]

$$h^*_{i,k} = h^*_{0,k} + \frac{x^*_i}{2} - \frac{1}{\pi}\sum_{j=0}^{n} k_{i,j} p^*_{j,k} \tag{27}$$

where,

$$k_{i,j} = \left(i-j+\frac{1}{2}\right)\Delta x^* \left(\ln\left(\left|i-j+\frac{1}{2}\right|\Delta x^*\right)-1\right) - \left(i-j-\frac{1}{2}\right)\Delta x^* \left(\ln\left(\left|i-j-\frac{1}{2}\right|\Delta x^*\right)-1\right) \tag{28}$$

The Newton-Raphson method has generally been applied to EHL problems, that is, the simultaneous solving procedure for both fluid film pressure, Eq. (25) and elastic deformation, Eq. (28). A typical solving process for the Newton-Raphson method is a Gaussian elimination procedure. In spite of its fast convergence characteristics, this method does not provide satisfactory results for high and transient loading conditions of EHL, and what is worse it needs a large array of computing variables. Therefore, if very detailed computations for a certain contact location of interest such as an outlet region over the Hertzian contact area are needed, then the number of computing grids is very limited for large allocations of variables in a matrix array with the Newton-Raphson method. As shown in the matrix form of equations, the scale of the grids (N) enlarges the system equation size by ~N^2. (See the Appendix.)

However, the multigrid multi-level method of full approximation scheme is preferred to the Newton-Raphson method, because of its numerical stability in a highly nonlinear partial differential equation such as the Reynolds equation with elastic deformation over the contact area [10]. In the multigrid multi-level method, a coarser grid is used to accelerate convergence of fine grid residuals, and a finer grid yields accuracy from the coarse grid equations as in Fig. 6. The grid relationship between coarse and fine grid is shown in Fig. 7 for full weighting restricting operation. In this study, the computation of film pressure over the contact area is performed with 4 level and 2V-cycle multigrid multilevel method. The residual of line contact Reynolds equation is expressed as below:

$$r_i^h = \frac{\partial}{\partial x^*}\left(\xi\frac{\partial p^*}{\partial x^*}\right) - \frac{\partial\left(\rho^* h^*\right)}{\partial x^*} - \frac{\partial\left(\rho^* h^*\right)}{\partial t^*} = 0 \tag{29}$$

where $\xi = \dfrac{\rho^* h^{*3}}{\eta^* \lambda}$ and $\lambda = \dfrac{12 u_s \eta_0 R_x^2}{a^3 p_H}$.

The time difference term of the Reynolds equation is discretized as Eq. (30) and the film pressure is updated to get δ_i^h at grid level h with relaxation factor ω_{gs}.

$$\left.\frac{\partial\left(\rho^* h^*\right)}{\partial t^*}\right|_j^k = \frac{\left(\rho^* h^*\right)\Big|_j^k - \left(\rho^* h^*\right)\Big|_j^{k-1}}{\Delta t^*}. \tag{30}$$

$$\bar{p}_i^{*h} = \tilde{p}_i^{*h} + \omega_{gs}\delta_i^h \tag{31}$$

The following equation is to be solved for the fluid film pressure in the direction of contact movement with the Gauss-Seidel iteration method:

$$A^i \delta_i^h = r^h \tag{32}$$

where

$$A_i^j = \frac{\partial\left(L^h p^{*h}\right)_i}{\partial p_j^{*h}}. \tag{33}$$

However, the area of Hertzian contact has very small value of ξ and it makes the computation of fluid film pressure diverge occasionally. In this case, Jacobi distributive relaxation is applied to this area and very stable convergence of the film pressure computation can be obtained as Eqs. (34) and (35).

$$A_i^j = \frac{\partial\left(L^h p^{*h}\right)_i}{\partial p_j^{*h}} - \frac{1}{2}\left(\frac{\partial\left(L^h p^{*h}\right)_i}{\partial p_{j+1}^{*h}} + \frac{\partial\left(L^h p^{*h}\right)_i}{\partial p_{j-1}^{*h}}\right) \tag{34}$$

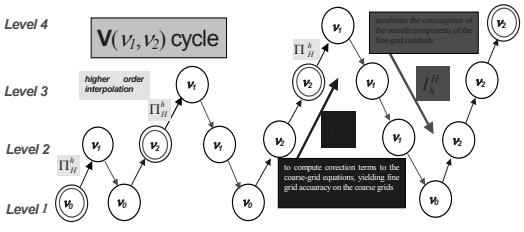

Fig. 6. Multigrid multilevel method for V cycle with Reynolds equation.

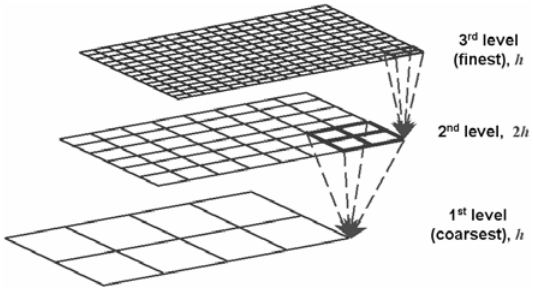

Fig. 7. Restricting grid matches in the multigrid multilevel method.

$$\overline{p}_i^{*h} = \tilde{p}_{i,j}^{*h} + \omega_{ja}\left(\delta_{i,j}^h - \left(\delta_{i+1}^h + \delta_{i-1}^h\right)/2\right) \quad (35)$$

According to the computational domain division by ξ value, system equations with Eqs. (31) and (32) are solved and if the value ξ is small, then Jacobi distributive relaxation method is applied with Eqs. (34) and (35).

All the time the summation of dimensionless pressures, ($p^* = E'b/4R$), over the grids matches with the applied contacting force W^* which comes from valve spring reactions due to valve lift. It is expressed in dimensionless form as below.

$$\int_{-\infty}^{\infty} p^*\left(x^*, t^*\right) - \frac{\pi}{2} = 0 \,. \quad (36)$$

4. Results and discussion

The computation of film thickness between cam and follower is performed for two types of followers, which are flat and rolling types. Both cases consider the effect of viscous damping in the valve spring. At 500rpm of camshaft speed, the valve spring force has a linear function to the valve lift, where the viscous damping does not appear so much as expected. On the other hand, the spring force shows highly nonlinear function to the valve lift shape at higher speed of 5000rpm, where the viscous damping is dominant (Fig. 8).

Under the contact geometry between cam and follower in the push-rod type valve train system, both dimensionless contact loads and entraining velocities of lubricant are computed for flat and rolling followers as shown in Figs. 9 and 10. The difference in the entraining velocity and loads comes from the contact spot geometries, mainly curvature of radius of contact point in the cams for flat and roller followers. The shape of contact loads in the roller follower is not in the absolute values that are the same as that of a flat follower. It is the dimensionless value W^* that is the function of curvature of the radius of the contact point, applied load and equivalent elastic modulus. Although the absolute load is the same as each other case, the contact geometry is totally different. Therefore, the dimensionless loads as shown in Figs. 9 and 10 cannot be the same in their dimensionless forms under their geometrical contact conditions. In the computations of those values, the viscous damping effect of the valve spring is included. In these figures, we can find very large differences in loads and entraining velocities of lubricant between flat and rolling followers, even under the same kinematic systems and operating conditions.

From these figures it can be easily seen that the entraining velocity in case of rolling follower is generally larger than that in case of flat follower except a certain short period. Therefore, it is inferred that the

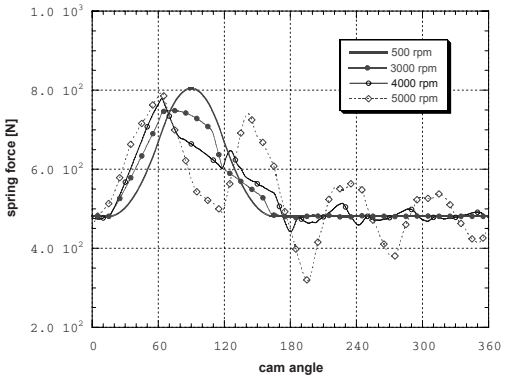

Fig. 8. Spring forces with viscous damping under several camshaft speeds.

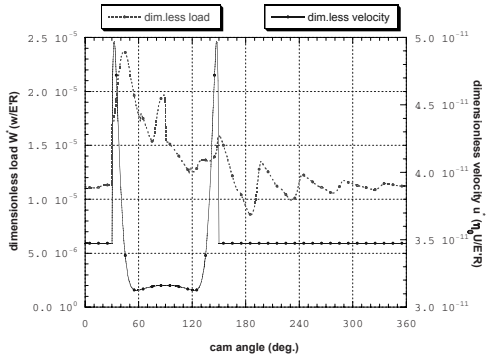

Fig. 9. Dimensionless velocities and loads for the contact between cam and flat follower at 3000rpm.

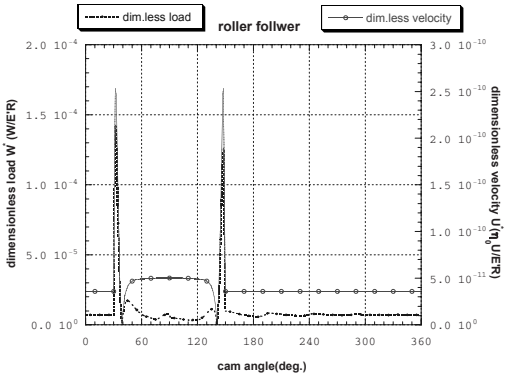

Fig. 10. Dimensionless velocities and loads for the contact between cam and rolling follower at 3000rpm.

film thickness of rolling follower should be thicker than that of flat follower with the lubrication aspects, which excludes the possibility of boundary lubrication with high friction and wear rate.

As shown in the Dowson-Higginson formula, Eq. 26, the film thickness is the function of load and contact speed. However, it is more dependent on the contact velocity $U^{*0.694}$ rather than the load $W^{*-0.128}$ as shown in the power digits such as 0.694 and -0.128. The digit for the contact speed is much higher than for the load as in Eq. 26. Therefore, the results that the film thickness is much higher in roller follower than in flat follower are in good accordance with the formula, Eq. (26).

The dynamic film which comes from the squeeze film effect is so great that ignoring it leads to an estimation of thicker film thickness than the actual film thickness. For the contact with a flat follower shown in Fig. 11 the dynamic film thickness is thinner than that of steady contact condition over the entire cycle. The minimum film thicknesses by Dowson-Hamrock's (D-H) formula show similar shapes to our computation results. However, this formula is very dependent upon the contact velocity rather than the applied load. From 30° to 50° and 130° to 150° of camshaft angle, the film thickness by D-H's shows sudden rises, whereas the dynamic film thickness in our computation is suppressed by the effect of relatively large load without any spikes during these periods.

For the contact with rolling follower in Fig. 11 the film thickness is thicker than that with flat follower during all of the engine cycle. This is the reason that rolling has its own rotational velocity, and therefore the entraining velocity of the lubricant is larger than that in the contact with the flat follower. Higher entraining velocity of lubricant makes thicker fluid film that removes the possibility of boundary lubrication. This is the reason that the rolling follower is widely used in order to reduce the abnormal frictional resistance and the wear rate. By comparing Figs. 11 with 12, it is found that the rolling follower has better tribological advantage than the flat follower. As it is also expected that high entraining velocity of lubricant becomes thicker, the dynamic film thickness of rolling follower is thicker than that of steady state entraining velocity of lubricant. On the other hand, D-H predicts thicker film thickness from 30° to 50° and 130° to 150° of camshaft angle when high entraining velocity occurs. This is the reason that the film thickness computed by D-H's does not include the squeeze film effect, so it shows large dependence only on the entraining velocity of lubricant itself.

The locations of minimum film thickness when the squeeze film effect is considered differ from the results when only steady condition is considered as shown in Fig. 13. The location of minimum film thickness under steady contact condition occurs near the exit region, which is a typical pattern for EHL, whereas it is located near the center of contact area under the dynamic loading condition. In our computation, it is found that the dynamic effect, $\partial(\rho h)/\partial t$, which is shown in the last term of the Reynolds equation, reduces the load capacity as well as changes the location of minimum film thickness of steady condition (Fig. 14).

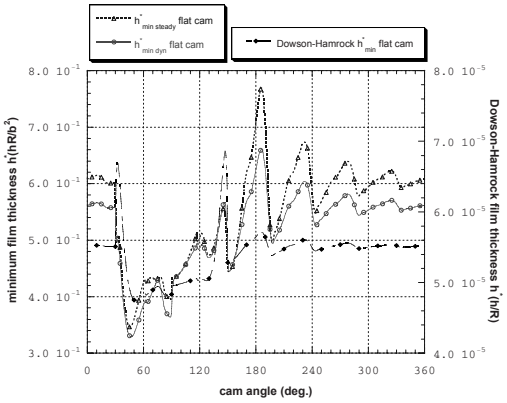

Fig. 11. Film thicknesses of dynamic, steady state and Dowson-Hamrock formula for flat follower at 3000rpm.

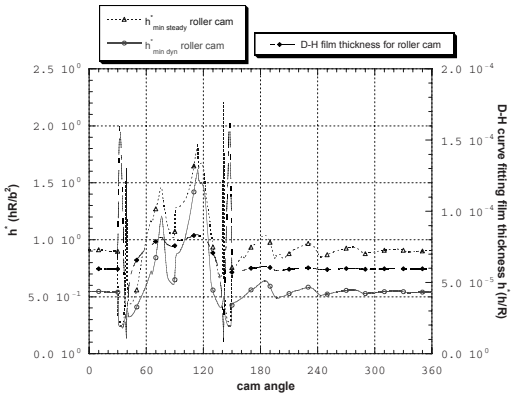

Fig. 12. Film thicknesses of dynamic, steady state and Dowson-Hamrock formula for rolling follower at 3000rpm.

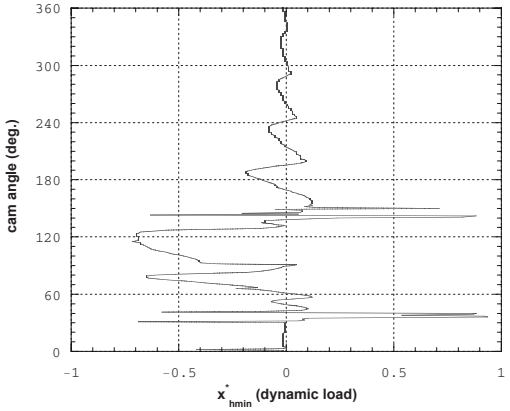

Fig. 13. Location of minimum film thickness under the dynamic velocity condition at 3000rpm for rolling follower.

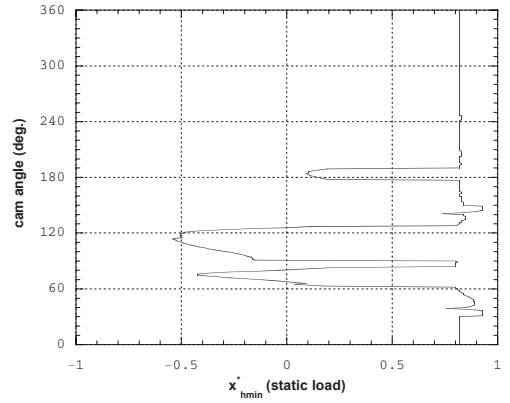

Fig. 14. Location of minimum film thickness under the steady velocity condition at 3000rpm for rolling follower

5. Conclusion

In this work, we have demonstrated the squeeze film effects which are generally not considered for the conventional EHL computations by comparing flat and rolling follower contacts with cam. Although the kinematic systems are all the same, the difference between contact geometries greatly influences both entraining velocities of lubricant and applied loads. In general, the rolling follower system produces a thicker film than a flat follower under the same condition of geometrical scale and operating condition. This means that rolling follower provides better tribological condition, which gives low wear possibility to cam and follower contacts.

The results are also compared with those by Dowson-Hamrock's formula which does not consider the dynamic film effect. Without the dynamic film effect, the minimum film thickness by D-H's formula is strongly dependent on the entraining velocity of lubricant, whereas the minimum film thickness, including the squeeze film effect, is dependent on the applied load.

Nomenclature

A : Area of the contact point, m^2
b : Half Hertzian length ($R\sqrt{8W/\pi}$), m
d : Diameter of spring wire, m
E : Young's modulus of surface, Pa
E' : Equivalent Young's modulus, Pa
$\frac{1}{E'}=\frac{1}{2}\left(\frac{1-\nu_a^2}{E_a}+\frac{1-\nu_b^2}{E_b}\right)$
F_s : Spring force, N
G : Material parameter in fluid film, $\alpha E'$
G' : Shear modulus in spring, N/m^2
h^* : Dimensionless film thickness, ($h\,R/b^2$) or (h/R) for Dowson-Hamrock formula
K : Spring constant, N/m
L : Developed length of the spring helix, m
N_c : Number of active spring coils
p^* : Dimensionless pressure, p/p_H
p_H : Hertzian pressure, $E'b/4R$, Pa
R : Equivalent radius of contact, m
R_r : Roller radius, m
R_c : Cam radius, m
r_i : Residual for Reynolds equation
u_c : Contact point velocity in the in the z direction, m/s
u_e : Entraining velocity of lubricant, m/s
u_s : Sliding velocity, m/s
u_t : Contact point velocity in the in the x direction, m/s
U^* : Dimensionless velocity, $u\eta_0/E'R$
w : Applied load, N
W^* : Dimensionless load, $w/E'R$
X_p : x component of center of the curvature of roller follower movement, m
x^* : Contact region coordinate to the sliding direction, x/b
y : Axial displacement of spring element, m
y_o : Maximum cam lift, m
Y_p : y component of center of the curvature of roller follower movement, m
r : Radius of spring, m
t : Time, s
α : Pressure-viscosity coefficient, m^2/N
α' : Wave speed, m/s

χ : Angle between contact point and valve lift direction
ε : Equivalent coefficient of viscous damping per unit length of the spring
ϕ : Angle of camshaft rotation
ϕ_p : Pressure angle, *rad*
η : Lubricant viscosity, $N\,s/m^2$
λ : Distance between cam axis and contact point, *m*
γ : Curvature of radius at contact point between cam and follower, *m*
ρ_m : Density at $dp/dx = 0$, Kg/m^3
ρ : Density of lubricant, Kg/m^3
ρ' : Density of spring material, Kg/m^3
σ : Curvature of radius, *m*
ξ : Curvilinear coordinate along spring length
ω : Angular speed of cam, *rad/s*

Superscript

* : Dimensionless variable

Acknowledgment

This work was supported by the Seoul Research and Business Development Program (Grant No. 10583) and by the ERC(CMPS) program of MEST/ KOSEF(Grant No.R11-2005-048-00000-0).

References

[1] P. K. Goenka, R. S. Paranjpe and Y.-R. Jeng, FLARE: An Integrated Package for Friction and Lubrication Analysis of Automotive Engines, (1992) SAE 92047.
[2] A. Dyson, Kinematics and Geometry of Cam and Finger Follower System, *Tribology International*, 13 (3) (1998) 121-132.
[3] J. Lee and D. J. Patterson, Nonlinear Valve Train Dynamics Simulation with a Distributed Parameter Model of Valve Springs, *Journal of Engineering for Gas Turbines and Power*, (119) (1997) 692-698.
[4] R. S. Paranjpe and B. A. Gecim, Comparative Friction Assessment of Different Valve-Train Types Using the FLARE Code, (1992) SAE 920491.
[5] R. S. Paranjpe, Dynamic Analysis of a Valve Spring with a Coulomb-Friction Damper, *Journal of Mechanical Design*, (112) (1990) 509-513.
[6] L. Houpert and B. J. Hamrock, Fast Approach for Calculating Film Thickness and Pressures in Elastohydrodynamically Lubricated Contacts at High Loads, *Journal of Tribology*, (108) (1986) 411-420.
[7] D. Dowson, C. M. Taylor and G. A. Zhu, Transient Elastohydrodynamic Lubrication Analysis of a Cam and Follower, *Journal of Physics*, (25) (1992) A313-A320.
[8] D. Dowson, P. Harrison and C. M. Taylor, The Lubrication of Automotive Cams and Followers, Mechanism and Surface Distress, 12th Leeds-Lyon Conference, (1985) 305-322.
[9] L. E. Scales, J. E. Rycroft, N. R. Horswill and B. P. Williamson, Simulation and Observation of Transient Effects in Elastohydrodynamic Lubrication, (1996) SAE 961143.
[10] A. Lubrecht, W. E. Napel and R. Bosma, Multigrid: An Alternative Method for Calculating Film Thickness and Pressure Profiles in Elastohydrodynamically Lubricated Line Contacts, *Journal of Tribology*, (108) (1986) 551-556.
[11] S. Hanachi and F. Freudenstein, The Development of a Predictive Model for the Optimization of High-Speed Cam-Follower Systems with Coulomb Damping Internal Friction and Elastic and Fluidic Elements, *Journal of Mechanisms, Transmissions and Automation in Design*, (108) (1986) 506-515.
[12] J. Matthews and F. Sadeghi, Kinematics and Lubrication of Camshaft Roller Follower Mechanics, *Tribology Transactions*, (39) (1996) 425-433.
[13] R. Stone and H. J. Leornard, Determination of the Instaneous Radius of Curvature of a Cam at the Contact Point with a flat Follower Moving Orthogonally, *Journal of Engineering Tribology*, (208) (1994) 147-149.
[14] C. M. Taylor, Engine Tribology, Elsevier, (1993).
[15] S. Jang and I. Suh, VI Improver's Effects on the Elastohydrodynamic Lubrication in Cam and Follower Contacts, (1999) SAE 1999-01-1221.
[16] S. Jang and K. Park, Dynamic EHL Film Thickness in Cam and Follower Contacts of Various Valve Lifts, *Advances in Powertrain Tribology*, (2000) 101-107.

Appendix

There are three basic unknowns for the line contact EHL problems with Newton-Raphson method as below:

$$\left(\rho_m^* h_m^*\right)^n = \left(\rho_m^* h_m^*\right)^o + \left[\Delta\left(\rho_m^* h_m^*\right)\right]^n \quad \text{(A-1)}$$

$$p_j^{*n} = p_j^{*o} + \left(\Delta p_j^*\right)^n \quad \text{(A-2)}$$

$$h_0^{*n} = h_0^{*o} + \left(\Delta h_0^*\right)^n \tag{A-3}$$

$\rho_m^* h_m^*$, p^* and h^* are the density multiplied by film thickness at the exit bound of contact area, film pressure and film thickness constant, respectively. The old known values subscripted by *o* are added by the differences from the computation results of Eq. (A-4), and then new values for the three unknowns subscripted by *n* are computed by equations from (A-1) to (A-3). Then the $\Delta\left(\rho_m^* h_m^*\right)$, Δp_j^* and Δh_0^* are now the unknowns for this problem and solved until their values are enough small under predefined limits. For each node *i,* the residual for line contact Reynolds equation is expressed as Eq. (A-4).

$$\left[\frac{\partial f_i}{\partial(\rho_m^* h_m^*)}\right]^o \left[\Delta\left(\rho_m^* h_m^*\right)\right]^n + \sum_{j=2,\ldots}^{N}\left(\frac{\partial f_i}{\partial p_j^*}\right)^o \left(\Delta p_j^*\right)^n + \left(\frac{\partial f_i}{\partial h_0^*}\right)^o \left(\Delta h_0^*\right)^n = -f_i^o \tag{A-4}$$

where $\left[\partial f_i / \partial\left(\rho_m^* h_m^*\right)\right]^o$, $\left[\partial f_i / \partial p_j^*\right]^o$, and $\left[\partial f_i / \partial h_m^*\right]^o$ are defined analytically [6] and f_i for line contact Reynolds equation is defined as below.

$$f_i = h_i^{*3}\left(\frac{dp^*}{dx^*}\right) - \frac{3\pi^2 U^*}{4W^{*2}}\eta_i^*\left(h_i^* - \frac{\rho_m^* h_m^*}{\rho_i^*}\right) \tag{A-5}$$

The constant dimensionless load is taken into account by

$$\int_{x_{\min}^*}^{x_{\max}^*}\left(\Delta p^*\right)^n dx^* = \frac{\pi}{2} - \int_{x_{\min}^*}^{x_{\max}^*} p^{*o} dx^* = \sum_{j=2,\ldots}^{N} C_j\left(\Delta p_j^*\right)^n = \left(\Delta W^*\right)^n \tag{A-6}$$

A linear system of N+1 equations for the unknowns $\Delta\left(\rho_m^* h_m^*\right)$, Δp_j^* and Δh_0^* are to be solved with the following matrix form:

$$\begin{bmatrix} \frac{\partial f_1}{\partial \rho_m^* h_m^*} & \frac{\partial f_1}{\partial p_2^*} & \cdots & \frac{\partial f_1}{\partial p_N^*} & \frac{\partial f_1}{\partial h_0^*} \\ \frac{\partial f_2}{\partial \rho_m^* h_m^*} & \frac{\partial f_2}{\partial p_2^*} & & \frac{\partial f_2}{\partial p_N^*} & \frac{\partial f_2}{\partial h_0^*} \\ \bullet & \bullet & & \bullet & \bullet \\ \frac{\partial f_N}{\partial \rho_m^* h_m^*} & \frac{\partial f_N}{\partial p_2^*} & & \frac{\partial f_N}{\partial p_N^*} & \frac{\partial f_N}{\partial h_0^*} \\ 0 & C_2 & & C_N & 0 \end{bmatrix}^o \begin{Bmatrix} \Delta\left(\rho_m^* h_m^*\right) \\ \Delta\left(p_2^*\right) \\ \bullet \\ \Delta\left(p_N^*\right) \\ \Delta\left(h_0^*\right) \end{Bmatrix}^n = \begin{Bmatrix} -f_1 \\ -f_2 \\ \bullet \\ -f_N \\ \Delta W' \end{Bmatrix}^o \tag{A-7}$$